World Academy of Science, Engineering and Technology
International Journal of Mechanical and Mechatronics Engineering
Vol:4, No:9, 2010

Study on the Mechanical Behavior of the Varactor of a Micro-Phase Shifter

Mehrdad Nouri Khajavi, Sajjad Ahoui Ghazvin, Ghader Rezazadeh and Mohammad Fathalilou

Abstract**—** In this paper static and dynamic response of a varactor of a micro-phase shifter to DC, step DC and AC voltages have been studied. By presenting a mathematical modeling Galerkin-based step by step linearization method (SSLM) and Galerkin-based reduced order model have been used to solve the governing static and dynamic equations, respectively. The calculated static and dynamic pull-in voltages have been validated by previous experimental and theoretical results and a good agreement has been achieved. Then the frequency response and phase diagram of the system has been studied. It has been shown that applying the DC voltage shifts down the phase diagram and frequency response. Also increasing the damping ratio shifts up the phase diagram.

Keywords**—**MEMS, Phase Shifter, Pull-in Voltage, Phase Diagram

I. Introduction

MICROELECTROMECHANICAL systems (MEMS) are increasingly gaining popularity in modern technologies, such as atomic force microscope (AFM), sensing sequence-specific DNA, and detection of single electron spin, mass sensors, chemical sensors, and pressure sensors [1,2]. MEMS devices are generally classified according to their actuation mechanisms. Actuation mechanisms for MEMS vary depending on the suitability to the application at hand. The most common actuation mechanisms are electrostatic, pneumatic, thermal, and piezoelectric [3]. Electrostatically actuated devices form a broad class of MEMS devices due to their simplicity, as they require few mechanical components and small voltage levels for actuation [3], which the electrostatic actuation is inherently non-linear. Microbeams (e.g., fixed-fixed and cantilever microbeams) under voltage driving are widely used in many MEMS devices such as capacitive micro-switches, micro phase shifters and resonant micro-sensors. These devices are fabricated, to some extent, in a more mature stage than some other MEMS devices. One of the most important issues in the electrostatically-actuated micro-devices is the pull-in instability. The pull-in instability is a discontinuity related to the interplay of the elastic and electrostatic forces. When a potential difference is applied between a conducting structure and a ground level, the structure deforms due to electrostatic forces. The elastic forces grow about linearly with displacement whereas the electrostatic forces grow inversely proportional to the square of the distance. When the voltage is increased the displacement grows until at one point the growth rate of the electrostatic force exceeds than the elastic force and the system cannot reach a force balance without a physical contact, thus pull-in instability occurs. The critical voltage is known as "pull-in voltage". Some previous studies predicted pull-in phenomena based on static analysis by considering static application of a DC voltage [4-5].

Phase shifters are key components of many communication and sensor systems. Most of existing phase shifters are based on semiconductor or ferrites technologies. High material and fabrication expenses, as well as high RF losses associated with the materials, hinder their applications [6]. Distributed MEMS transmission line (DMTL) phase shifter was first proposed by Barker and Rebeiz [7] using a quartz substrate .A series of MEMS airgap bridge varactors are placed over a coplanar waveguide (CPW) transmission line. Phase shifts are created by phase velocity changes induced by altering bridge parallel-plate capacitances.

There are two classes of RF MEMS phase shifters namely analog and digital. The analog phase shifters provide a continuous variable phase shift from 0 to 360° using varactor capacitive switches [7]; whereas the digital phase shifters provide a discrete or quantized set of phase delays with 1 bit 180°, 2 bit 180°/90° set of delay networks which allow phase shifts of 0, 90, 180 and 270° depending on the combination of bits used [8]. When comparing to the other topologies, the distributed MEMS transmission line (DMTL) phase shifter on silicon wafer has the advantage of low cost, low loss and small size. In addition, the DMTL phase shifters demonstrated in this work have better performance [9] on simple coplanar waveguide (CPW) transmission lines because CPW based phase shifters are uniplanar. This is one of the main advantages as only one side of the substrate is used; eliminating the need for via-hole process and simplifying the fabrication and integration process with other components[10].

Though the phase shifting technique has many advantages, it is marred by a few inaccuracies due to the vibration and mechanical movement of the phase shifter itself. Much of the

F. A. Author is with the Islamic Azad University of Takestan, Iran (email: mehrdadnouri@ieee.org)

S. B. Author, Islamic Azad University of Takestan, Iran. He is now with the Department of Mechanical Engineering (ah_orga3@yahoo.com).

T. A. Author is with the Mechanical Engineering Department, Urmia University (e-mail;g.rezazadeh@urmia.ac.ir)

F. A. Author is with the Mechanical Engineering Department, University of Tabriz, Iran (e-mail: m.fathalilou@tabrizu.ac.ir, corresponding author to provide phone: +98-914-363-6714).

work reported to compensate these errors, to our knowledge, is on the theoretical side of the process. Not much work has been done to eliminate these errors [11]. One method to eliminate these errors was first conceived by Smyth and more in their work of instantaneous phase shifting interferometry (IPSI) [12].

In spite of the many research about the phase shifters, the mechanical behavior of the phase shifters had not been studied generally yet. In this paper, theoretically, is studied the mechanical behavior of the micro-capacitor used as a varactor. By applying a mathematical modeling and numerical solution, the static and dynamic response of the system to the DC, AC and a combination of these voltages is investigated. It is researched the effects of residual, thermal and the stretching stresses on the dynamic and static instability of a micro-varactor. Also, it is studied the frequency response of the system for various applied DC voltage and the phase diagram for the first natural frequency and different damping ratios. Finally, the effect of the assumed DC voltage on the phase shifting is investigated.

I. Mathematical Modeling

Fig. 1 shows the schematic view of the circuit of the phase shifter given in reference of [6]. In this paper it is focused on the mechanical behavior of the varctor of fig. 1 shown clearly in fig. 2.

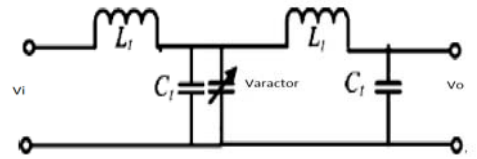

Fig. 1. A schematic view of the phase shifter circuit [6]

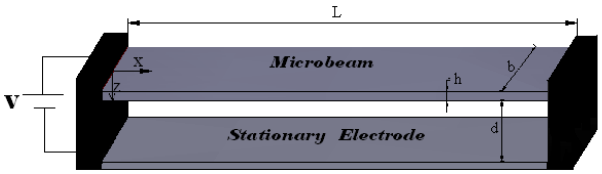

Fig. 2. Schematic view of an electrostatically actuated fixed-fixed microbeam

The governing equation of motion for the transverse displacement of the beam $w(x, t)$ actuated by an electrostatic load of voltage V is written as:

$$EI\frac{\partial^4 w}{\partial x^4}+\rho bh\frac{\partial^2 w}{\partial t^2}+c\frac{\partial w}{\partial t}=\frac{\varepsilon b}{2}\left(\frac{V}{d-w(x,t)}\right)^2 \quad (1)$$

where $\widetilde{E}$ is dependent on the beam width b and film thickness h. A beam is considered wide when $b \geq 5h$. Wide beams exhibit plane-strain conditions, and therefore, $\widetilde{E}$ becomes the plate modulus $E/(1-\upsilon^2)$, where E and υ are the Young's modulus and Poisson's ratio, respectively. A beam is considered narrow when $b < 5h$. In this case, $\widetilde{E}$ simply becomes the Young's modulus, E. $I=\left(bh^3/12\right)$ is the effective moment of inertia of the cross-section which is wide relative to thickness and width, ρ is density, ε and d are the dielectric constant of the gap medium and initial gap, respectively. The microbeam is subject to a viscous damping, which can be due to squeeze-film damping. This effect is approximated by an equivalent damping coefficient c per unit length [5]. The boundary conditions of the microbeam are written as follow:

$$w(0,t)=w(L,t)=0,\ \frac{\partial w}{\partial x}(0,t)=\frac{\partial w}{\partial x}(L,t)=0 \quad (2)$$

A. Stretching Stress Effect

Fixed-fixed microbeams represent an example of microstructure suffering from the geometric nonlinearity midplane stretching. When a beam is in bending, the actual beam length L' is longer than the original length L, although there is no displacement in the x direction at the beam ends. The actual length along the center line of the beam is calculated by integrating the arc length ds along the curved beam based on the cubic shape functions for small deflection of beam, $w(x)$:

$$L'=\int_0^L ds \approx \int_0^L \sqrt{1+\left(\frac{dw}{dx}\right)^2}\,dx \quad (3)$$

Considering $L >> w$, hence $(dw/dx)^2 << 1$, as a result, the elongation is approximately given by:

$$\Delta L \approx \frac{1}{2}\int_0^L \left(\frac{dw}{dx}\right)^2 dx \quad (4)$$

Therefore the stretching stress and force are given by:

$$\sigma_a=\frac{\widetilde{E}}{2L}\int_0^L \left(\frac{dw}{dx}\right)^2 dx, \quad \text{and} \quad N_a=bh\,\sigma_a \quad (5)$$

B. Residual Stress Effect

Residual stress, due to the inconsistency of both the thermal expansion coefficient and the crystal lattice period between the substrate and thin film, is unavoidable in surface micromachining techniques. Accurate and reliable data for residual stress are crucial to the proper design of MEMS devices that are related to these techniques [13,14]. Considering the fabrication sequence of MEMS devices, residual force can be expressed as:

$$N_r=\sigma_r(1-\upsilon)bh \quad (6)$$

where σ_r is the biaxial residual stress [15], and υ is the Poisson's ratio. Assuming the stretching and residual stresses effects, the governing differential equation takes the following form:

$$\widetilde{EI}\frac{\partial^4 w}{\partial x^4}+\rho bh\frac{\partial^2 w}{\partial t^2}+c\frac{\partial w}{\partial t}-\left[N_a+N_r\right]\frac{\partial^2 w}{\partial x^2}=\frac{\varepsilon b}{2}\left(\frac{V(t)}{d-w(x,t)}\right)^2 \quad (7)$$

For convenience in analysis, this equation must be non-dimensionalized.In particular, both the transverse displacement, *w*, and the spatial coordinate, *x* , are normalized by characteristic lengths of the system and thegap size and beam length,respectively,accordingto: $\hat{w}=w/d$ and $\hat{x}=x/l$ .Tim is non-dimensionalized byacharacteristicperiodofthesystemaccordingto: $\hat{t}=t/t^*$ with $t^*=\left(\rho bhL^4/\widetilde{EI}\right)^{1/2}$.

Substituting these parameters into Eq. (7), the following nondimensional equation is obtained:

$$\frac{\partial^4 \hat{w}}{\partial \hat{x}^4}+\frac{\partial^2 \hat{w}}{\partial \hat{t}^2}+\hat{c}\frac{\partial \hat{w}}{\partial \hat{t}}-\left[\hat{N}_a+\hat{N}_r\right]\frac{\partial^2 \hat{w}}{\partial \hat{x}^2}=\alpha_1\left(\frac{\hat{V}(t)}{1-\hat{w}(\hat{x},\hat{t})}\right)^2 \quad (8)$$

The non-dimensional parameters appeared in Eq. (8) are:

$$\alpha_1=\frac{6\varepsilon L^4}{\widetilde{E}h^3d^3},\quad \hat{c}=\frac{12cL^4}{\widetilde{E}bh^3t^*},\quad \hat{N}_a=\frac{12N_aL^2}{\widetilde{E}bh^3},$$
$$\hat{N}_r=\frac{12N_rL^2}{\widetilde{E}bh^3} \quad (9)$$

II. Numerical Solution

A. Static Analysis

In the static analysis there is no exist time derivatives, so using Eq. 8 the governed equation describing the static deflection of the microbeam can be obtained as follow:

$$L(\hat{w}_s,V)=\frac{d^4\hat{w}_s}{d\hat{x}^4}-\left[\hat{N}_a+\hat{N}_r\right]\frac{d^2\hat{w}_s}{d\hat{x}^2}-\alpha_1\left(\frac{\hat{V}}{1-\hat{w}_s(\hat{x})}\right)^2=0 \quad (10)$$

where the $\hat{w}_s(\hat{x})$ for fixed-fixed end microbeam must be satisfied same boundary condition as mentioned in Eq. (2). Due to the nonlinearity of derived equation, the solution is complicated and time consuming. Direct applying Galerkin based reduced order model create a set of nonlinear algebraic equation. In this paper we use a method to solve it which consists of two steps. In first step, we use step by step linearization method (SSLM), and in second, Galerkin method for solving the linear obtained equation is used. Because of considerable value of $\hat{w}$ respect to initial gap especially when the applied voltage increases, the linearizing respect to $\hat{w}$, may cause some considerable errors, therefore, to minimize the value of errors, the method of step-by-step applied voltage increasing is proposed and the governing equation is linearized at each step [16]. To use SSLM, it is supposed that the $\hat{w}^k{}_s$, is the displacement of beam due to the applied voltage V^k . Therefore, by increasing the applied voltage to a new value, the displacement can be written as:

$$\hat{w}_s^{k+1}=\hat{w}_s^k+\delta\hat{w}=\hat{w}_s^k+\psi(\hat{x}) \quad (11)$$

when

$$V^{k+1}=V^k+\delta V \quad (12)$$

Therefore, Eq. (10) can be rewritten as follow:

$$\frac{d^4\hat{w}_S^{K+1}}{d\hat{x}^4}-\left[\hat{N}_a^{K+1}+\hat{N}_r\right]\frac{d^2\hat{w}_S^{K+1}}{d\hat{x}^2}-\alpha_1\left(\frac{V^{K+1}}{1-\hat{w}_S^{K+1}}\right)^2=0 \quad (13)$$

By considering small value of δV , it is expected that ψ would be small enough, hence using of Calculus of Variation Theory and Taylor's series expansion about $\hat{w}^k$, and applying the truncation to first order of it for suitable value of δV , it is possible to obtain desired accuracy. The linearized equation to calculate ψ can be expressed as:

$$L(\psi)=\frac{d^4\psi}{d\hat{x}^4}-\left[\hat{N}_a^k+\delta\hat{N}_a+\hat{N}_r\right]\frac{d^2\psi}{d\hat{x}^2}-\delta\hat{N}_a\frac{d^2\hat{w}}{d\hat{x}^2}\left(\hat{w}^k,V^k\right)-2\alpha_1\frac{\left(V^k\right)^2}{\left(1-\hat{w}_s^k\right)^3}\psi-2\alpha_1\frac{V^k\delta V}{\left(1-\hat{w}_s^k\right)^3}=0 \quad (14)$$

where variation of the hardening term based on Calculus Variation Theory can be expressed as:

$$\delta\hat{N}_a=\int_0^1\left(\frac{d^2\hat{w}}{d\hat{x}^2}(\hat{w}^k,\hat{V}^k)\right)\psi(\hat{x})d\hat{x} \quad (15)$$

By considering small value of δV^ and as a result $\psi(\hat{x})$,multiplying $\delta\hat{N}_a$ to $d^2\psi/d\hat{x}^2$ would be small enough that can be neglected. The obtained linear differential equation is solved by Galerkin based reduced order model. $\psi(\hat{x})$ based on function spaces can be expressed as:

$$\psi(\hat{x})=\sum_{j=1}^{\infty}a_j\varphi_j(\hat{x}) \quad (16)$$

where $\varphi_j(\hat{x})$ is the *i*th shape function that satisfies the boundary conditions. The unknown $\psi(\hat{x})$, is approximated by truncating the summation series to a finite number, *n*:

$$\psi_n(\hat{x})=\sum_{j=1}^{\infty}a_j\varphi_j(\hat{x}) \quad (17)$$

By substituting the Eq. (17) into Eq. (14), and multiplying by $\varphi_i(\hat{x})$ as a weight function in Galerkin method and then integrating the outcome from $\hat{x}=0$ to 1 , the Galerkin based reduced-order model is generated.

B. Dynamic Analysis

In the numerical solution it is considered that the microbeam is deflected by a DC voltage, V_{DC} and then the dynamic characteristics and forced response of the system considered about these conditions. So total deflection of the microbeam consists of two parts as:

$$\hat{w}(\hat{x},\hat{t}) = \hat{w}_s(\hat{x}) + \hat{w}_d(\hat{x},\hat{t}) \tag{18}$$

$\hat{w}_s(\hat{x})$ introduces the static deflection of the beam and $\hat{w}_d(\hat{x},\hat{t})$ denotes the dynamic deflection about $\hat{w}_s(\hat{x})$.

Because of the applied AC voltage in the model is small enough than DC voltage $V_{AC} << V_{DC}$ by linearizing Eq. 8 about calculated $\hat{w}_s(\hat{x})$ small linear vibrations are studied by following equation:

$$\frac{\partial^4 \hat{w}}{\partial \hat{x}^4} + \frac{\partial^2 \hat{w}}{\partial \hat{t}^2} + \beta \frac{\partial \hat{w}}{\partial \hat{t}} = \frac{\alpha (v_s + v_d)^2}{(1-\hat{w})^2} = \frac{\alpha v_s^{\,2}}{(1-w_s)^2} + \frac{2\alpha v_s}{(1-w_s)^2}\delta v + \frac{2\alpha v_s^{\,2}}{(1-w_s)^3}\delta w \tag{19}$$

where $\delta V = V_{AC}$ and $\delta w = w_d$: The V_{AC} is small AC voltage and equal to $V_0 \sin(\omega t)$ and ω is excitation frequency.

Subtracting Eq. 19, the linearized equation of motion about equilibrium position can be obtained in the following form:

$$\frac{\partial^4 \hat{w}_d}{\partial \hat{x}^4} + \frac{\partial^2 \hat{w}_d}{\partial \hat{t}^2} + \hat{c}\frac{\partial \hat{w}_d}{\partial \hat{t}} - \frac{2\alpha v_{DC}^{s\,2}}{(1-w_s)^3} w_d = \frac{2\alpha V_{DC}^s V_0 \sin(\omega t)}{(1-w_s)^2} \tag{20}$$

In order to solve this equation, a Galerkin based reducedorder model can be used [17]. So $\hat{w}_d$ can be expressed as:

$$\hat{w}_d(\hat{x},\hat{t}) = \sum_{j=1}^{\infty} T_j(\hat{t})\varphi_j(\hat{x}) \tag{21}$$

where $\varphi_j(\hat{x})$ is the jth shape function that satisfies the boundary conditions. The unknown $\hat{w}_d(\hat{x},\hat{t})$; can be approximated by truncating the summation series to a finite number, N:

$$\hat{w}_d(\hat{x},\hat{t}) = \sum_{j=1}^{N} T_j(\hat{t})\varphi_j(\hat{x}) \tag{22}$$

In this paper, $\varphi_j(\hat{x})$ is selected as the jth undamped linear mode shape of the straight microbeam. By substituting the Eq. 22 into Eq. 20 and multiplying by $\varphi_i(\hat{x})$ as a weight function in Galerkin method and then integrating the outcome from $\hat{x}=0$ to 1; the Galerkin based reducedorder model is generated as:

$$\sum_{j=1}^{n} M_{ij}\ddot{T}_j(\hat{t}) + \sum_{j=1}^{n} C_{ij}\dot{T}_j(\hat{t}) + \sum_{j=1}^{n}\left(K_{ij}^{mech} - K_{ij}^{elec}\right)T_j(\hat{t}) = F_i \sin(\omega t) \tag{23}$$

where $\overline{M}, \overline{C}, \overline{K}^{mech}$ and $\overline{K}^{elec}$ are mass, damping, mechanical and electrical stiffness matrixes, respectively. Also $\overline{F}$ introduces the forcing vector. The mentioned matrices and vector are given by:

$$M_{ij} = \int_0^1 \varphi_i \varphi_j \, d\hat{x} \qquad C_{ij} = \hat{c}\int_0^1 \varphi_i \varphi_j \, d\hat{x}$$

$$F_i = \int_0^1 \frac{2\alpha V_{DC}^{s} V_0 \sin(\omega t)}{(1-w_s)^2}\varphi_i \, dx$$

$$K_{ij}^{elec} = \int_0^1 \frac{2\alpha V_{DC}^{s\,2}}{(1-w_s)^3}\varphi_i \varphi_j \, d\hat{x} \tag{24}$$

$$K_{ij}^{mech} = \int_0^1 \varphi_i \varphi_j^{iv} \, d\hat{x}$$

The same procedure is used to study the response of the system to the step DC voltage, where the equation 23 is written as follow:

$$\sum_{j=1}^{n} M_{ij}\ddot{T}_j(\hat{t}) + \sum_{j=1}^{n} C_{ij}\dot{T}_j(\hat{t}) + \sum_{j=1}^{n} K_{ij}^{mech} T_j(\hat{t}) = F_i \tag{25}$$

where F introduces the forcing vector as follow:

$$F_i = \int_0^1 F(V, \ddot{\hat{w}})\phi_i d\hat{x} \qquad i,j=1,..,n \tag{26}$$

Now, equation 25 can be integrated over time by various integration methods such as Rung-Kuta method where $\ddot{\hat{w}}(\hat{x},\hat{t})$ in each time step of integration take the value of previous step.

By applying the procedures mentioned, the static and dynamic stabilities and frequency response of the system is gained.

C. Phase Diagram

It is known that there is a phase shifting, φ between the applied AC voltage and harmonic vibration of the microbeam. For study the phase diagram under various damping ratios and DC voltages the following formula is applied:

$$\tan \varphi = \frac{2\xi\left(\frac{\omega}{\omega_n}\right)}{1-\left(\frac{\omega}{\omega_n}\right)^2} \quad (27)$$

where ω_n and ω are fundamental and excitation frequency of the system. ξ is the damping ratio. The fundamental frequency is varied by variable DC voltage.

III. Results & Discussion

For verification of our numerical solution it is considered a microbeam with the geometric and material properties listed in table 1.

TABLE I THE VALUES OF DESIGN VARIABLES

Design Variable	Value
B	$50\mu m$
H	$3\mu m$
D	$1\mu m$
E	169GPa
ρ	2331kg/ m^3
ε	8.85PF/m
V	0.06

In table 2 and 3 it is compared the calculated pull-in voltage with previous works for the fixed-fixed and cantilever microbeams with properties of table 1, respectively.

TABLE II COMPARSION OF THE PULL-IN VOLTAGE FOR A FIXED-FIXED MICROBEAM

	Residual stress (MPa)	Our residual	Energy model [18]	MEMCAD [18]
L=350	0 100 -25	20.1V 35.3V 13.8V	20.2V 35.4V 13.8V	20.3V 35.8V 13.7V
L=250	0 100 -25	39.5V 57.3V 33.4V	39.5V 56.9V 33.7V	40.1V 57.6V 33.6V

TABLE III COMPARSION OF THE PULL-IN VOLTAGE FOR A CANTILEVER MICROBEAM ($L = 150\mu m$)

	Our result	Cosolve simulation [18]	Closed form 2D model [18]
Pull-in Voltage(v)	17.0	16.9	16.8

It is shown that the calculated pull-in voltages are in good agreement with previous works. For validation of dynamic results with previous works, a fixed-fixed microbeam is considered with the specifications of the pressure sensor used by Hung and Senturia [19]:

E =149 GPa , $\rho = 2330kg/m^3$, $L = 610\mu m$, $b = 40\mu m$, $h = 2.2\mu m$ and $d = 2.3\mu m$.

Because h is given as a nominal value, it is modified to match the experimental pull-in voltage .Accordingly, thickness is obtained $h = 2.135\mu m$. They have considered a residual stress of -3.7 MPa.

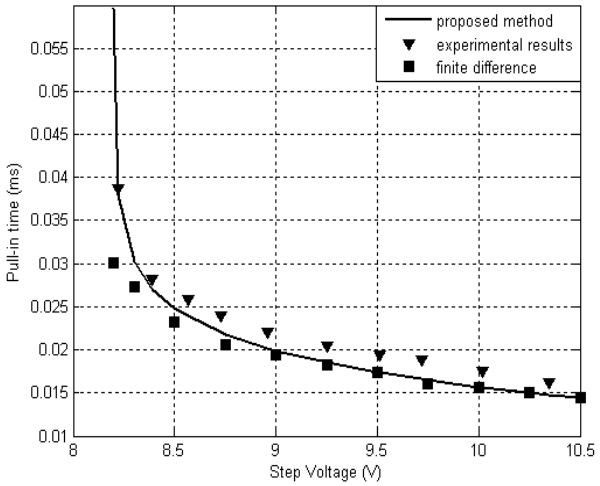

Fig. 3. Comparison of the pull-in time for no damping case without the stretching effects.

In fig. 3 the calculated pull-in time obtained using proposed method is compared with the theoretical and experimental results of Hung and Senturia [19] for various values of step DC voltage. The pull-in time is found by monitoring the beam response over time for a sudden rise in the displacement; at that point the time is reported as the pull-in time [20]. As figure 2 illustrates, calculated results are in excellent agreement with the theoretical and experimental results. It is shown that for no damping case before V= 8.18 V the pullin instability dos not occur, so this step DC voltage can be introduced as dynamic pull-in voltage for the microbeam.

Figure 4 illustrates the frequency response of the system for various DC voltages. It is shown that increasing the DC

voltage shifts left the frequency diagram. Because, increasing the DC voltage decreases the stiffness and consequently the fundamental frequency of the system. Also due to the decreasing of the stiffness, maximum amplitude of the microbeam increases. Also, the rate of the frequency shifting and amplitude increasing is raised near the pull-in voltage. This can be due to the higher rate of stiffness decreasing near the pull-in voltage

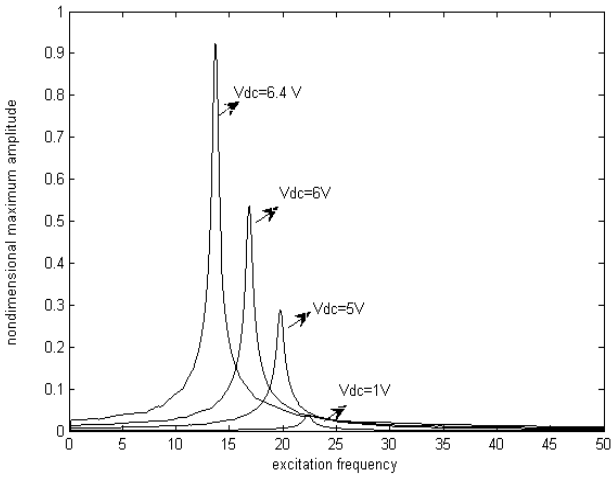

Fig. 4. the frequency response of the system for various Vdc

Figure 5 shows the phase diagram of the system versus various damping ratio. It is shown that the higher damping shifts right the diagram. In figure 6, it is illustrated that by increasing the applied DC voltage phase diagram shifts left.

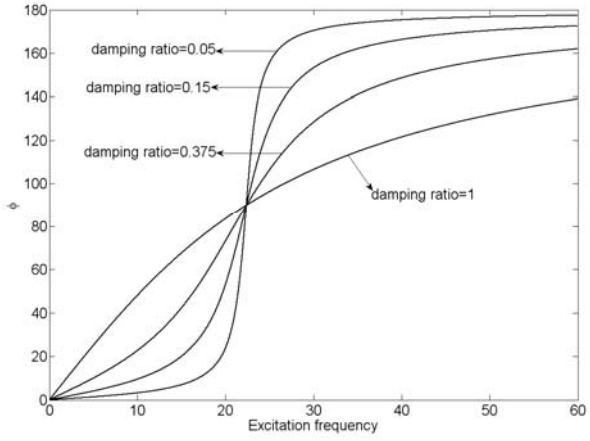

Fig. 5. Phase Diagram for Various Damping Ratios

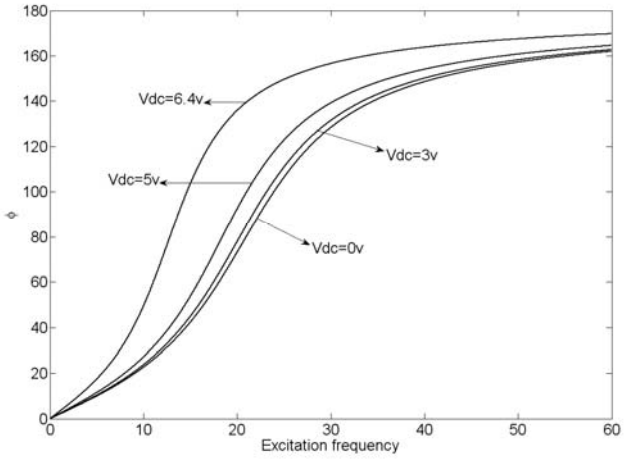

Fig. 6. Comparison of the pull-in time for no damping case without the stretching effects.

IV. Conclusion

In the presented work static and dynamic response of a micro-vaactor of a phase shifter to DC, step DC and AC voltages were studied. By presenting a mathematical modeling Galerkin-based step by step linearization method (SSLM) and Galerkin-based reduced order model were used to solve the governing static and dynamic equations, respectively. Then by applying these methods static and dynamic pull-in voltages were obtained and validated by previous experimental and theoretical results and a good agreement were achieved. It was shown that applying a DC voltage shifts left the frequency response. It was concluded that it can be due to the decreasing of the total stiffness of the system. Finally, the effects of the applied DC voltage and damping on the phase diagram were studied. It was illustrated that the DC voltage and damping ratio shifts down and up this diagram, respectively.

Then the frequency response and phase diagram of the system has been studied. It has been shown that applying the DC voltage shifts down the phase diagram and frequency response. Also increasing the damping ratio shifts up the phase diagram.

References

[1] M Basso., L Giarre., M.Dahleh, I. Mezic, Numerical analysis of complex dynamics in atomic force microscopes, In: *Proceedings of the IEEE International Conference on Control Applications,* Trieste, Italy, 1-4 September: 1026- 1030,1998.

[2] A. Nabian, Gh.Rezazadeh, M.Haddad-Derafshi, A.Tahmasebi, Mechanical behavior of a circular micro plate subjected to uniform hydrostatic and non-uniform electrostatic pressure, *Microsystem Technologies* 14: 235 240,2008.

[3] S.Senturia, *Microsystem Design*, Kluwer, Norwell, MA, USA. , 2001

[4] Gh.Rezazadeh, H.Sadeghian, E.Abbaspour, A comprehensive model to study nonlinear behaviour of multilayered micro beam switches, *Microsystem Technologies*, 14(1): 143,2008 .

[5] E.M.Abdel-Rahman, M.I.Younis, A.H.Nayfeh, Characterization of the mechanical behavior of an electrically actuated microbeam, *Journal of Micromechanical Microengineering* **12**: 759-766.2002.

[6] Letter to Editor, , "A distributed MEMS phase shifter on a low-resistivity silicon substrate", Sensors and Actuators A 144, 207–212, 2008.

[7] N.S. Barker, G.M. Rebeiz, Distributed MEMS true-time delay phase shifters and wide band switches, IEEE Trans. Microw. Theory Tech. 46 (11) , 1881–1890, 1998.
[8] J.S. Hayden, G.M. Rebeiz, , 2-Bit MEMS distributed X-band phase shifters, IEEE Microwave Guided Wave Lett. 10 (12), 540–542,2000.
[9] J.S. Hayden, A. Malczewski, J. Kleber, C.L. Goldsmith, G.M. Rebeiz, , 2 and 4-Bit DC 18 GHz microstrip MEMS distributed phase shifters, in: IEEE MTT-S International Microwave Symposium Digest, Phoenix, USA, pp. 219–222, 2001.
[10] W. Palei, A.Q. Liu , A.B. Yu, A. Alphones, Y.H. Lee, , "Optimization of design and fabrication for micromachined true time delay (TTD) phase shifters"Sensors and Actuators A, 119, 446–454, 2005.
[11] B.K.A.Ngoi , K.Venkatakrishnan, N.R.Sivakumar , T.Bo, , "Instantaneous phase shifting arrangement for microsurface profiling of flat surfaces.optics communications 190, 109-116,2001.
[12] R . Smythe, R. More , , Instantaneous phase measuring interferometry, Optical Engineering 23(4), 361-365,1984.
[13] T.Mukherjee, G.K. Fedder, White J., Emerging simulation approaches for micromachined devices, *IEEE Transaction Computer Aided Design Integr Circuits Syst* 19: 1572-1589 , 2000 .
[14] S.D.Senturia, N.Aluru, J.White, Simulating the behavior of MEMS devices, *IEEE Comput Sci Eng* **4**(1): 30-43 , 1997.
[15] R.K.Gupta, Electrostatic pull-in test structure design for in-situ mechanical property measurement of microelectromechanical systems (MEMS), Ph.D. dissertation, MIT, Cambridge, MA, 10-27 , 1997.
[16] Gh.Rezazadeh, A.Tahmasebi, M. Zubtsov, Application of piezoelectric layers in electrostatic mem actuators: Controlling of pull-in voltage, *Microsystem Technologies* 12(12): 1163-1170 , 2006.
[17] H.Nayfeh, Mook Nonlinear Oscillations. New York. Wiley,1979.
[18] Gh. Rezazadeh, M. Fathalilou, K. Shirazi, S. Talebian, "A Novel Relation between Pull-in Voltage of the Lumped and Distributed Models in Electrostatically-Actuated Microbeams", MEMSTECH', 22-24 April,2009,Polyana-Svalyava(Zakarpattya), UKRAINE, 31-35,2009.
[19] E. S. Hung and S. D. Senturia ,"Generating efficient dynamical models forMicroelectromechanical systems from a few finite-element simulation runs", journal of Microelectromechanical Systems, vol. 8, pp. 280-289. 1999.
[20] M. I. Younis, E. M. Abdel-Rahman, A. Nayfeh ,"A Reduced-Order Model for Electrically Actuated Microbeam-Based MEMS", journal ofMicroelectromechanical systems, vol. 12, no. 5, pp. 672-680, 2003.